Solar Energy 227 (2021) 625–634

Contents lists available at ScienceDirect

Solar Energy

journal homepage: www.elsevier.com/locate/solener

Energy and economic assessment of floating photovoltaics in Spanish reservoirs: cost competitiveness and the role of temperature

Leonardo Micheli

Advances in PV technology Research Group (AdPVTech), University of Jaén, Jaén, Spain

ARTICLE INFO

Keywords:
Floating PV modules
Energy cost
Spain
Cooling
Economics

ABSTRACT

The installation of photovoltaic modules on water bodies, known as floating photovoltaics (FPV), addresses one of the main issues arising with the growing deployment of photovoltaics: land occupancy. However, while the FPV capacity is increasing exponentially, its economics is still being debated, as few field data are nowadays available and discussions on the expected performance are still ongoing. This work presents a first estimate of the maximum capital expenditures that FPV installers should target to make these systems as profitable as optimally tilted in-land photovoltaic (LPV) plants. The analysis is conducted by estimating and comparing the modelled Levelized Cost Of Energy (LCOE) and Net Present Value (NPV) of potential FPV and LPV systems in Spain. The analysis shows that low-inclination FPV systems are not expected to outperform optimally tilted LPV in terms of energy yield. However, FPV can already compete with LPV in Spain in terms of lifetime cost of electricity and profits if the expected lower operating temperatures are confirmed. The maximum allowed capital expenditure is found to vary depending on the location. The impact of factors influencing the energy and economic performance of FPV is also discussed, with particular attention to the effect of the improved thermal behavior expected from FPV systems.

1. Introduction

Spain has been the major photovoltaic (PV) installer in Europe since the end of 2018. The national PV capacity has gone from 4.7 GW in December 2018 to 8.9 GW in just one year and to 11.7 GW in two years (REE, 2020). In 2020, PV produced 6.1% of the annual electrical energy generation, 70% more than in 2019 (REE, 2020), pushed by both the significant capacity installed in 2019 and by a temporary drop in electricity demand (Micheli et al., 2021). Spain's Integrated National Energy and Climate Plan 2021–2030 (Gobierno de España, 2020) targets to reach 39 GW of PV installed nationwide by 2030, more than three times the current capacity. Renewables are expected to provide 74% of the national electrical energy in 2030, with the aim of achieving 100% by 2050.

One of the main challenges associated with the global expansion of PV (and of renewables in general) is the land requirement, as these technologies have lower power densities than conventional sources (Capellán-Pérez et al., 2017). The 10 largest PV plants in Spain occupy, on average, approximately 2 ha (0.02 km^2) of land per MW (Álvarez and Zafra, 2021). If this trend is maintained, the objectives of the Integrated National Energy and Climate Plan will require, at a rate of almost 3 new GW of PV installed per year, the conversion of 60 km^2 of land into solar parks every year. Some issues related to the growing renewables' land occupancy have already been experienced in Spain. The high request has made the cost of PV land raise and, according to a recent estimation (Aparicio, 2020), it is currently up to 10 times more profitable renting land for installing PV rather than for farming. Also because of this, the cost of utility-scale PV in Spain is now higher than in other countries, especially for sites located nearby grid connection points (Ford, 2019). In addition, a recent letter from Spanish researchers to Science has warned about the potential effects that a large PV deployment can have on the biodiversity if the ecological value of the land is not adequately evaluated (Serrano et al., 2020).

One of the arising solutions that can address the land occupancy issues is floating PV (FPV), in which PV modules are installed on the surface of water bodies rather than on land. FPV still represents a small portion of the global PV capacity, but it has been growing exponentially since 2010 (Rosa-Clot and Tina, 2020a). By August 2020, FPV had reached a global 2.6 GW capacity (Haugwitz, 2020), twice the capacity reported at the end of 2018 (Rosa-Clot and Tina, 2020a). In Spain, the first grid-connected FPV system was opened in summer 2020 (Molina, 2020).

E-mail address: lmicheli@ujaen.es.

https://doi.org/10.1016/j.solener.2021.08.058
Received 8 June 2021; Received in revised form 16 August 2021; Accepted 19 August 2021
Available online 22 September 2021

Several factors, in addition to the reduced land occupancy, are pushing the deployment of FPV (Rosa-Clot and Tina, 2020b). For example, thanks to the shading that the modules produce, FPV can reduce the water evaporation rates, making more water available for hydroelectric, irrigation or drinking uses (Sahu et al., 2016). In addition, the same shading also reduces the risk of abnormal growth of algae, which can be dangerous to fish and lead to foul-smelling emissions (Gorjian et al., 2021).

On the other hand, because of its early stage of deployment, the economics of FPV are still being debated, as few and sometime contradictory data are available. Some authors have been sharing economic data for specific sites or regions. For examples, a recent work showed that the investments on FPV in Iran can be paid back in no more than 6 years (Fereshtehpour et al., 2021). Two different studies have estimated similar payback periods for FPV and silicon land-based (LPV) systems in Thailand and in Brazil (Cromratie Clemons et al., 2021; Padilha Campos Lopes et al., 2020). However, some authors have reported higher installation costs for FPV compared to ground-mounted plants (Rollet, 2020). This is not surprising as nowadays FPV has the same global capacity that conventional PV reached in 2003 (left plot of Fig. 1). In this light, the growing deployment of new FPV capacity can be expected to lead to significant cost reductions in future thanks to the economy of scale and to the maturing of the technology (Rosa-Clot and Tina, 2020c). The right plot of Fig. 1 shows the reduction in installation costs experienced by PV since 2010, when the global PV capacity was about 5% of todays' capacity. Part of this reduction is due to the drop in modules' price and to the raise in modules' efficiencies, and therefore it is common to both LPV and FPV installations. However, IRENA attributes the installation cost drop also to the decreasing balance of system costs, results of the experience learnt by the LPV market players and of the development of the supply chain structures (IRENA, 2020). A similar scenario can also be expected for FPV as the installed capacity grows. For example, recent works (Fereshtehpour et al., 2021; Rosa-Clot and Tina, 2020c) have shown that the cost of floating structures still has a significant weight in the FPV economics, due to its relatively young age, and can be expected to lower in future. In addition, higher costs of land, such as those experienced in Spain, might lower the gap between the capital costs of FPV and land-based PV (LPV), and favor the installation of FPV (Sahu et al., 2016). The need of no major site works, such as laying of foundations required by land-based PV, can additionally lower the capital costs of FPV (World Bank Group et al., 2018). Last, the use of existing electricity infrastructures in hydroelectric reservoirs can further lower the FPV installation costs compared to LPV (Haugwitz, 2020), even if this hybridization is still at an early stage of development (World Bank Group et al., 2018). All these factors can positively affect the Capital Expenditure (CAPEX) of FPV, reducing their Balance of System costs, increasing their profits and lowering their cost of electricity compared to traditional LPV.

In addition to expenditures, a full cost and profitability analysis of FPV should take into account also the factors directly affecting the energy production. For example, FPV systems are typically installed at lower tilts to reduce the effect of wind uplift and drifting (Ferrer-Gisbert et al., 2013; Silvério et al., 2018). This, however, makes FPV more subject to angular/reflection losses, reduces the in-plane irradiance and, therefore, limits the energy yield (El Hammoumi et al., 2021). On the other hand, though, most authors in the scientific literature (Dörenkämper et al., 2021; Liu et al., 2018; Sahu et al., 2016) have reported lower operating temperatures for FPV modules compared to LPV. These have been typically attributed to the proximity to water and, if confirmed, would lead to higher energy performance (see also 2.2).

So, while the deployment of FPV is already a profitable investment, it might not be as profitable as LPV yet. The scope of this work is identifying the maximum CAPEX that would make FPV systems economically competitive with in-land PV, taking into account the different conditions in which they operate. The motivation behind this investigation relies on the expectation of lower CAPEX achievable by floating PV in future thanks to the easier installation and decommissioning, to the potential hybridization with hydroelectric plants and to the reduced cost of land. In particular, the potential of floating PV is investigated by studying the reservoir surface availability in Spain, the fastest-growing PV market and one of the highest irradiation country in Europe. The energy performance is modelled taking into account location-specific irradiance and weather conditions and typical FPV and LPV configurations. Referenced data on capital and operational expenditures are used, along with long-term electricity price forecasts, to evaluate the economics and the profitability of FPV systems over their lifetime. The analysis makes use of and compares two common economic metrics, the Levelized Cost Of Energy (LCOE) and the Net Present Value (NPV). Particular attention is given to the positive benefits that lower module temperatures can give to floating PV compared to conventional systems. The impact of

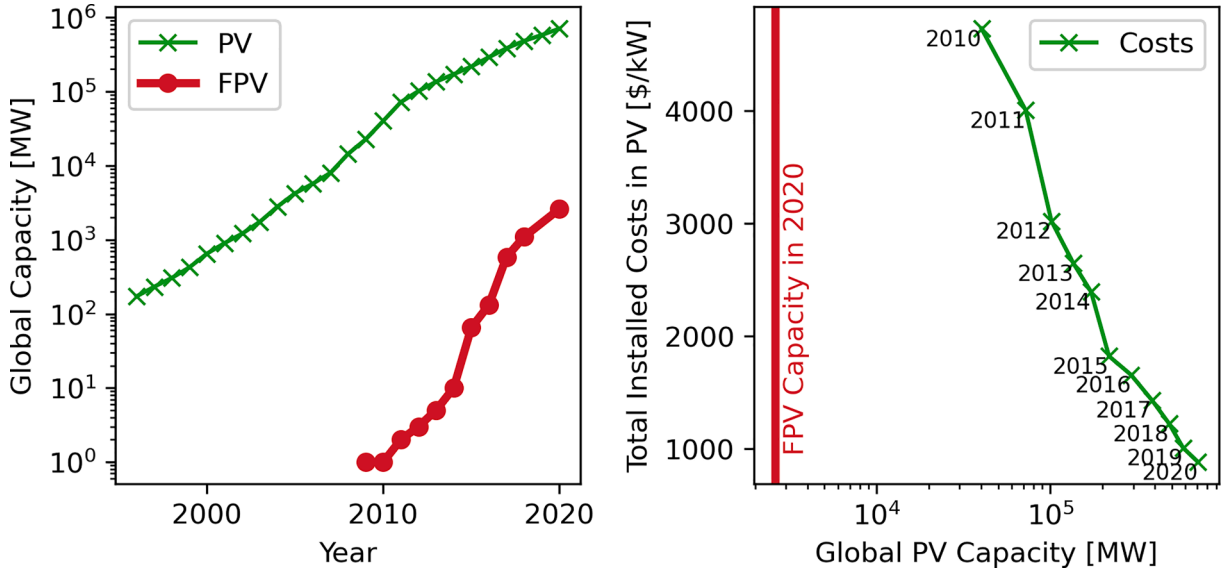

Fig. 1. Left plot: Evolution of cumulative PV and floating PV (FPV) capacities installed worldwide. Right plot: total installed costs for utility-scale systems vs. cumulative capacity. The red vertical lines mark the current FPV capacity. Yearly PV capacities sourced from (BP p.l.c., 2021). 2009 to 2018 FPV capacities sourced from (World Bank Group et al., 2018). August 2020 FPV capacity reported by (Haugwitz, 2020). Total installed costs sourced from (IRENA, 2020). (For interpretation of the references to color in this figure legend, the reader is referred to the web version of this article.)

additional factors on the FPV economics, such as the extra hydroelectric production achievable through water evaporation savings, is also analytically investigated.

2. Materials and methods

2.1. Reservoir data

This work takes into account as potential FPV sites the reservoirs listed in the Global Reservoir and Dam Database (GRanD) v1.3 (Lehner et al., 2011). This is the same database used by the World Bank to assess the global FPV potential (Fox, n.d.). It contains a large number of information on each dam. However, it is acknowledged that it might report only part of the total number of dams available in the country (Mulligan et al., 2020), leading therefore to a conservative estimation of the surface available for FPV.

FPV plants typically occupy only a portion of the reservoir's surface (A_{FPV}). This quota is expressed in % (r_{FPV}), and varies from site to site. For example, the new FPV system opened in 2020 in Spain covers 0.07% of the reservoir where it is installed (Molina, 2020). Thailand's first FPV plant covers 37% of its pond (Deboutte, 2021). The largest FPV system in the UK covers 10% of a reservoir near London (Lightsource bp, 2016). The Brazilian FPV systems analyzed in (Silvério et al., 2018) cover between 0.25 and 3.58% of their reservoirs. In this work, different scenarios are considered, described in 3.1.

In addition, rows of non-horizontal PV modules have to be distanced to avoid mutual shadings. In this work, a spacing between rows 20% larger than the height of the modules from the ground has been considered. The calculation was conducted considering also that, while a horizontal PV module occupies a surface as large as its area, a tilted module occupies a $\cos\theta$ fraction of its area. So, given a reservoir of surface A_{FPV}, the maximum achievable FPV capacity for a given r_{FPV} cover ratio was calculated as follows:

$$P_{FPV} = A_{FPV} \bullet r_{FPV} \bullet \frac{1}{\cos\theta + 1.2 \bullet \sin\theta} \bullet \eta \bullet 1000 \mathrm{W/m^2} \quad (1)$$

where θ is the tilt angle of the FPV modules and η their electrical conversion efficiency (21.4%).

2.2. PV performance model

Hourly PV performance have been simulated using a model implemented in Python 3.7 and exploiting the functions available in pvlib python (Holmgren et al., 2018). The potential PV output of each location was calculated using the PVWatts DC power model (Dobos, 2014), and applying a fixed 10% loss to convert the modelled DC output into AC. The model required in input the effective irradiance, calculated using hourly data downloaded from CAMS (Copernicus Atmosphere Monitoring Service, n.d.; Lefèvre et al., 2013; Gschwind et al., 2019; Qu et al., 2017) and already corrected taking into account the angle of incidence losses (De Soto et al., 2006). The ground diffuse and sky diffuse components of irradiance were calculated using the models in (Loutzenhiser et al., 2007) and in (Hay and Davies, 1980), respectively, and assuming a fixed albedo of 0.25.

The cell temperature was estimated using the PVsyst model (PVsyst SA, n.d.), based on the Faiman equation (Faiman, 2008):

$$T_c = T_a + \frac{POA \bullet \alpha \bullet (1 - \eta)}{U_0 + U_1 \bullet ws} \quad (2)$$

where T_a is the ambient temperature downloaded from (Buchhorn et al., 2020; Inness et al., 2019), POA is the plane-of-array irradiance, α is the absorption coefficient of solar irradiation (set to 0.9), η is the module efficiency (fixed to 0.214), U_0 is the constant heat transfer component, U_1 is the convective heat transfer component and *ws* is the wind speed. Often, including in this case, a single constant heat loss coefficient is considered: $U = U_0 + U_1 \bullet ws$. The higher the U-value, the better the thermal exchange of the PV module with the environment, and, therefore, the lower its operating temperature.

Dörenkämper et al. (Dörenkämper et al., 2021) measured the thermal behaviors of five FPV systems deployed in Netherlands and Singapore and compared them with those of land-based systems. They distinguished between "open structures" (where the back of the FPV module faced the water surface) and "close structures" (where the back of the FPV module faced the floater's surface). They reported U-values:

- of 55 and 57 W/m^{2}K for two open structure FPV systems (tracked and 10° tilted respectively),
- between 36 and 41 W/m^{2}K for three close structure FPV systems (tilt angles in between 10° and 17°).

Liu et al. (Liu et al., 2018) analyzed the performance of FPV systems of different designs installed in a reservoir in Singapore. They found average U-values of 46, 35 and 31 W/m^{2}K for free-standing, small footprint and large footprint FPV designs, respectively. Kjeldstad et al. (Kjeldstad et al., 2021) reported a U-value as high as 71 W/m^{2}K for FPV modules in direct-contact with water ($\theta = 0°$) and highlighted the need of using water temperature rather than ambient temperature in the calculation.

While most of the authors have been reporting and expecting improved thermal performance for FPV modules, Peters and Nobre (Peters and Nobre, 2020) showed similar temperatures for a floating PV system and a roof-mounted PV system located on a small building few meters away of the water basin shore. Supported also by the results of a simulation, they suggested that the reductions of temperature previously reported for FPV were possibly only an indirect effect of presence of the water. Water bodies, indeed, might influence the local ambient temperature or wind conditions, which are the factors responsible for the temperature of the PV modules, if these are not in direct contact with water. So, they concluded that one could expect similar thermal behaviors for PV systems located either on or nearby a water basin. This is also in agreement with the findings of (Dörenkämper et al., 2021), which reported for an open rack free standing LPV system installed 250 m of the shore a U-value of 39 W/m^{2}K. This was significantly higher than that of a deep inland rooftop system (27 W/m^{2}K) and similar to that of a nearby FPV with close structure (37 W/m^{2}K). For a different rooftop system located away from the water in Singapore, they reported a U-value of 31 W/m^{2}K instead. This is in line with the typical U-value for LPV (29 W/m^{2}K), employed, for example, by PVsyst (PVsyst SA, n.d.).

The aim of this paper is to investigate the potential economics of FPV compared to that of a conventional in-land (LPV) system, taking into account various possible thermal behaviors. As a baseline scenario, the FPV system is modelled as made of south-oriented and 10° tilted Si modules. Temperature coefficient of -0.0034 C^{-1} and electrical efficiency of 21.4% have been considered (Trina, 2021). The modules are modelled as if they were mounted on an open structure, where the backside of the modules faces the water surface. For this reason, a U-value of 56 W/m^2 is assumed as baseline, average of the U-values reported by (Dörenkämper et al., 2021) for FPV on open structures. However, it is acknowledged that this is among the highest U-values reported in the literature and, for this reason, a sensitivity analysis is also presented in Section 3.3. The 10° tilt for FPV was chosen as this was the maximum recommended for Spain by (Silvério et al., 2018). The comparison is conducted considering fixed LPV modules at optimum tilt and southward orientation with U-value of 29 W/m^{2}K. A discussion on the variability of each of the modelled factors is also reported in the paper.

2.3. Economics

The economics of FPV and LPV are quantified through the Levelized Cost of Electricity (LCOE) and the Net Present Value (NPV). The first

index is used to quantify the cost of producing a kWh of electricity and has been calculated as in (Micheli et al., 2020):

$$LCOE = \frac{CAPEX + \sum_{t=0}^{T} \frac{OMEX \cdot (1-Tx) \cdot (1+r_{om})^t}{(1+d)^t} - \sum_{t=0}^{N_d} \frac{D_n \cdot Tx}{(1+d)^t}}{\sum_{t=0}^{T} \frac{E_t \cdot (1-R_D)^t}{(1+d)^t}} \quad (3)$$

where T is total number of years of operation, $OMEX$ is the yearly operation and maintenance expenditure and r_{om} is the rate at which it varies every year (equal to the inflation rate), d is the discount rate, Tx is the income tax, E_t is the AC energy yield profile, and R_D is the system-level degradation rate. D_n is the annual tax depreciation for the PV plant, which allows recovering part of the investment cost through reduced taxes for a given period of time (Nd). In this work, depreciation has been modelled as linear and constant (Jiménez-Castillo et al., 2020). The values of all the parameters are shown in Table 1. E_t is calculated as average of daily values in the years 2010–2020.

The NPV expresses the profitability of an investment and has a positive value if the investment has returned a profit. The NPV has been calculated as follows (Micheli et al., 2020):

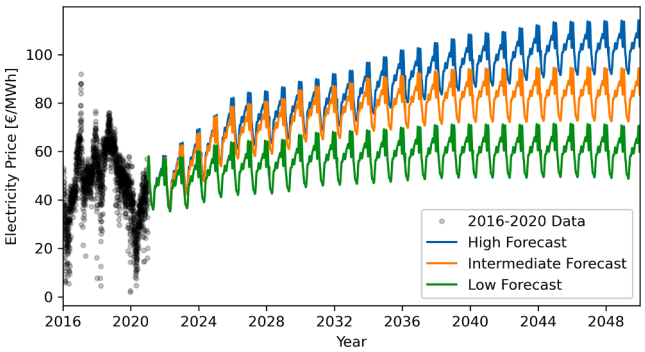

Fig. 2. Historical electricity price data and 2020–2050 forecast scenarios for Spain. Data for 2016–2020 sourced from (OMIE, n.d.). Forecasts sourced and adapted from (Perez-Linkenheil, 2019) using the Facebook Prophet algorithm (Taylor and Letham, 2017). The High scenario assumes a slow increase in renewable energies. The Low scenario assumes increases in renewable energies and in commodity prices, and stagnating CO_2 prices.

$$NPV = -CAPEX + \sum_{t=0}^{T} \frac{\sum_{i}^{365} (p(i) \cdot E_t(i)) \cdot (1-R_D)^t \cdot (1-Tx) - OMEX \cdot (1-Tx) \cdot (1+r_{om})^t}{(1+d)^t} + \sum_{t=0}^{N_d} \frac{D_n \cdot Tx}{(1+d)^t} \quad (4)$$

where p is the electricity price and the product $p(i) \cdot E_t(i)$ represents the gross revenues made per day (i) from selling the energy. Most of the electricity in Spain is sold through the Iberian Electricity Market, where the prices are set depending on the available energy volumes and costs and on the demand. Commercial forecasts estimate that the electricity prices will likely increase in future (Mazzoni and Manuell, 2019; Perez-Linkenheil, 2019), for at least a decade. The present work considers three electricity price scenarios reported in (Perez-Linkenheil, 2019), which forecast different price trends in Europe by 2050 (Fig. 2). Where not otherwise stated, this work uses the Intermediate scenario, which assumes increases in renewable energies and CO_2 prices (strong) and stagnating commodity prices. The trends are adjusted through (i) the addition of the seasonal component, extracted with Facebook Prophet (Taylor and Letham, 2017) from the 2010–2019 data (OMIE, n.d.), and (ii) the addition of a constant offset to make forecasts and actual values match at the start of 2021. It should be noted that the present work considers the average day-ahead electricity prices, not including taxes or grid access fees.

The goals of this work are (i) the estimation of the CAPEX that FPV should target to equalize the LCOE and the NPV of LPV systems, and (ii) the analysis of the factors affecting the energy and economic performance of FPV. So, the analysis is conducted by calculating the maximum CAPEX allowed for FPV to meet these conditions:

$$LCOE_F(CAPEX_F) \leq LCOE_L(CAPEX_L) \quad (5)$$

$$NPV_F(CAPEX_F) \geq NPV_L(CAPEX_L) \quad (6)$$

where the subscript F refers to floating PV systems and L refers to conventional land based PV systems. $CAPEX_L$ is fixed to 700 €/kW as reported in recent literature (IEA PVPS, 2020). The energy yields of the two PV configurations are calculated taking into account the aforementioned U-values and tilt angles of 10° for FPV, as recommended by (Silvério et al., 2018), and equal to the latitude for LPV. The baseline calculation assumes the same albedos and the same annual operational expenditure for both FPV and in-land PV.

3. Results

3.1. FPV capacity in Spain

The Global Reservoir and Dam Database (GRanD) v1.3 (Lehner et al., 2011) counts 262 dams in Spain, for a total reservoir surface of 1604 km^2. If fully occupied, this could ideally allocate up to 288 GW of PV modules installed at 10° tilt, distributed as shown in the left plot of Fig. 3. About 50% of the listed reservoirs have irrigation as main purpose, while the 28% of the reservoirs are used mainly for hydroelectricity. These hydropower basins could host 80 GW of the 288 GW.

Table 1
Economic parameters, sourced from (Micheli et al., 2020).

Parameter	Symbol	Value	Units	References
Annual escalation rate of the OMEX	r_{om}	1.23	%/year	(Micheli et al., 2020)
Capital Expenditure	CAPEX	700 (for LPV)	€/kW	(IEA PVPS, 2020)
Depreciation period	Nd	20	years	(Jiménez-Castillo et al., 2020)
Discount Rate	d	6.4	%/year	(Talavera et al., 2019)
Income Tax	Tx	25	%	(Talavera et al., 2019)
Linear system degradation	R_D	1.0	%/year	(Theristis et al., 2020)
O&M costs	OMEX	15	€/KW/year	(Talavera et al., 2019)
Years of operation	T	25	years	

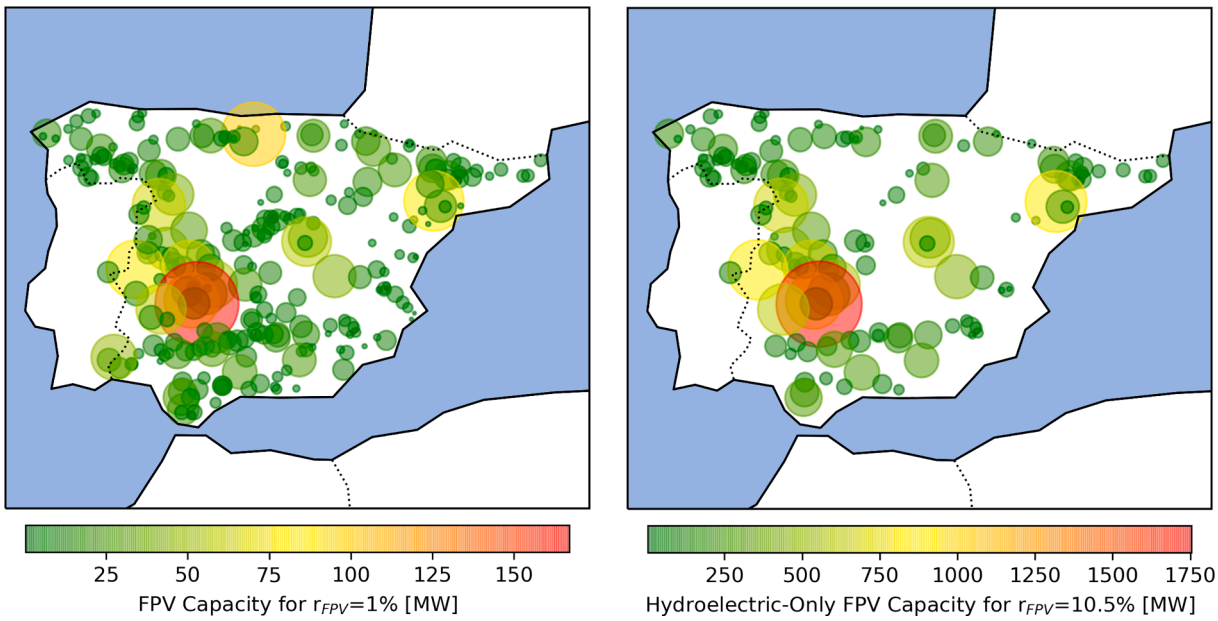

Fig. 3. Potential FPV site distribution and capacity for 1% r_{FPV} of all the reservoirs in Spain and for 10.5% r_{FPV} of only the basins with hydroelectric infrastructure (i.e. with hydropower production as primary or secondary purpose). Markers are sized and colored according to the FPV capacity that the reservoir they are highlighting could host. List of reservoirs sourced from (Lehner et al., 2011). (For interpretation of the references to color in this figure legend, the reader is referred to the web version of this article.)

However, an additional 23% of the dams are reported to have hydroelectric generation as second purpose, raising the potential capacity to 194 GW.

In reality, one can expect FPV not to cover the 100% of the reservoirs' surface. Installing FPV systems on only 1% of the available reservoir surface would already increase the current national PV capacity by 25%. In this configuration, the larger site would have a capacity of 167 MW, the smallest of 0.23 MW. Almost 30% of sites would have size >10 MW and more than 90% >1 MW. The 25% of the total FPV capacity will be concentrated in just 8 sites (3% of the total) and the 50% in 30 sites (11.5%). More than 45% of the potential FPV capacity would be located in Extremadura and Andalucía, two of the regions with the highest irradiation. In between 2016 and 2020, Spain consumed on average 263 TWh of electricity per year (REE, 2020). In the considered configuration (1% r_{FPV}), FPV could supply 1.7% of this demand.

Gorjian et al. (Gorjian et al., 2021) suggested a FPV coverage in between 40 and 60% to limit the abnormal growth of algae that might occur in some basins. If a 50% coverage is assumed, the maximum FPV capacity would raise to 144 GW, about 1.3 times the national installed capacity and 13 times more than the current PV capacity. This could cover 87% of the national energy demand.

Even if only few examples currently exist and more research on this solution has been recommended by previous researchers (Lee et al., 2020), the hybridization with hydropower is often mentioned as a

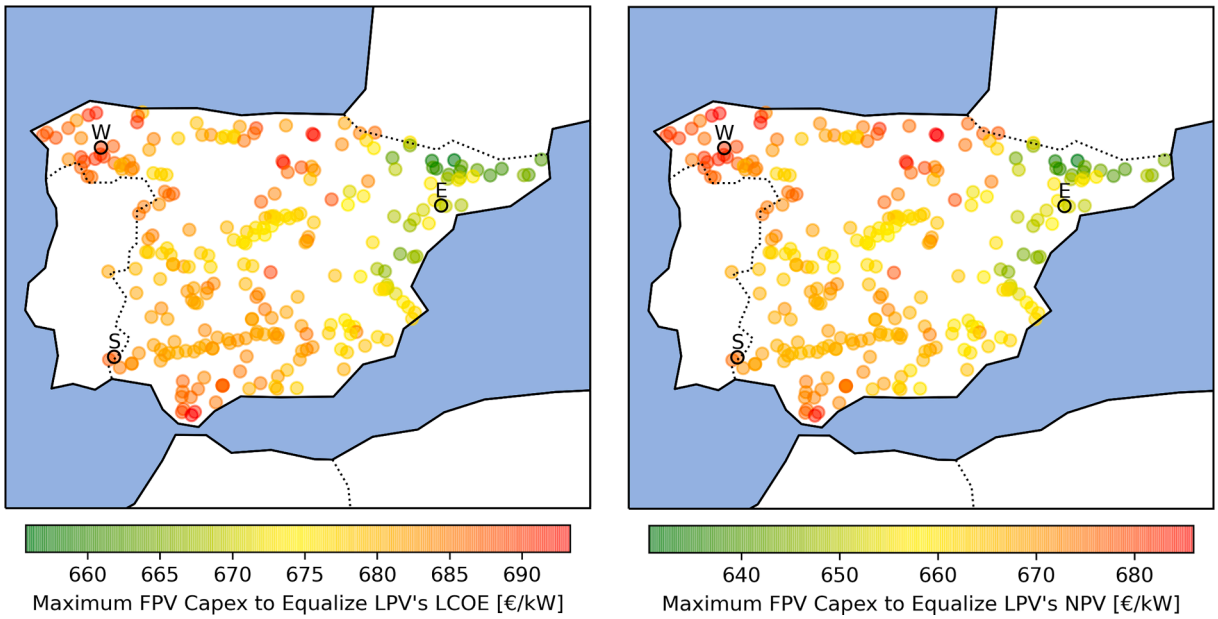

Fig. 4. FPV Installation Costs to achieve the same LCOE (left) and NPV (right) than conventional PV. CAPEX of LPV systems set to 700 €/kW. The letters "W", "S" and "E" mark the location of the three representative sites in the Western, Southern and Eastern regions described in Table 2.

potential benefit of FPV (Cazzaniga et al., 2019). For this scenario, it has been recommended to size the FPV systems as the hydropower plants where they are installed, so that FPV could use the existing electrical infrastructure (Fang et al., 2017). At the end of 2020, there were 20 GW of hydroelectric power in Spain. This means that the hydroelectric basins could host an additional 20 GW of PV: 75% of the capacity currently missing to reach the 2030 target for PV. This FPV capacity, shown in the right plot of Fig. 3, would provide 12% of the national energy demand, covering the 10.5% of the national hydropower basin surface available in (Lehner et al., 2011).

3.2. Economics of FPV vs. Land based PV

The maps in Fig. 4 show the maximum CAPEX that FPV should target to meet the LCOEs (left plot) and the NPVs (right plot) of in-land photovoltaics across Spain. At the given conditions, in order to reach the same LCOE, the CAPEX of FPV should in between 1.0 and 6.3% lower than that of LPV, depending on the location. Similarly, in order to get the same profits as in-land PV, FPV owners have to reduce the CAPEX by 2.0–9.9%. This lower CAPEX could be achieved, for example, through reduced costs of floaters, reduced land fees, and/or reduced installation/decommissioning costs. One should also consider that, according to equation (1), each kW of PV installed at 10° tilt requires ~80% of the land required at 30° tilt.

The results in Fig. 4 demonstrate that FPV, in some regions, can already compete with LPV from an economic perspective. Since the results vary with the location, three representative sites were selected among all the hydropower dams to facilitate the discussion on the potentials of FPV in the various regions of Spain. These are the largest reservoirs in each of the three regions at the extremities of the country: Galicia (West), Andalucía (South) and Cataluña (East). The results specific to these locations are reported in Table 2 and agree with the trends shown in Fig. 4. First, the maximum FPV CAPEX in the southernmost regions of Spain are close to the current LPV CAPEX. These are also the regions with the highest temperatures and energy yields and with significant reservoir surface availability. Second, high CAPEX allowances are also found on the northwest, probably results of the low irradiance conditions, which minimize the difference between the most performing and the less performing modules. On the other hand, the northeastern regions would require the strongest reduction in CAPEX (≥2.3% for LCOE and ≥3.8% for NPV). These are indeed the areas experiencing the lowest ambient temperatures and intermediate irradiance values. In these conditions, FPV is not expected to benefit significantly of the increased thermal exchange it can achieve.

It should be noted that the results in Fig. 4 do not evaluate the absolute economic value of FPV in each location. Indeed, they only show the difference in costs and revenues between LPV and FPV systems. The southern regions have both the highest CAPEX allowance and the best economic performance (i.e. lowest LCOE and highest NPV). However, for other locations, smaller differences do not necessarily translate in highest absolute profits or lower costs. For example, the northwest FPV systems have high CAPEX allowances, but the minimum economic returns. This is due to the lower irradiance experienced in this region, which minimizes the difference between LPV and FPV, but which also reduces the energy yield and therefore the profits.

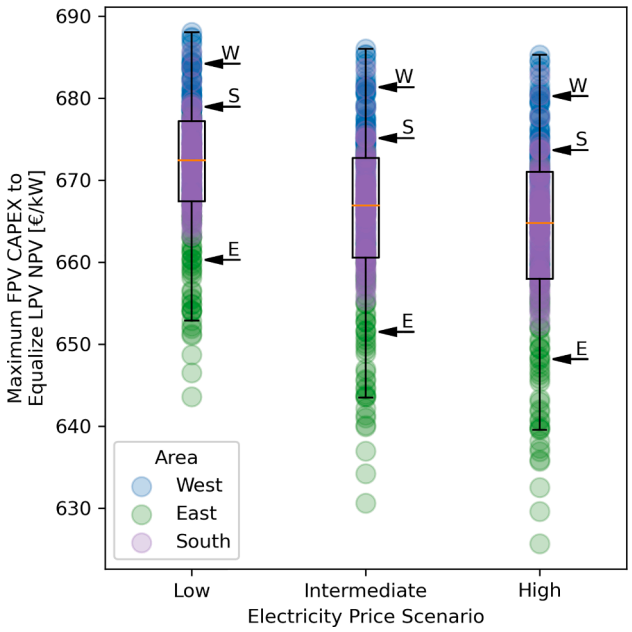

Fig. 5. Maximum CAPEX required by FPV to equalize the NPV of LPV. CAPEX of LPV set to 700 €/kW. Each data point represents one of the locations in (Lehner et al., 2011). Each location is color coded according to the area it belongs: East (Aragon, Cataluña, Valencia); South (Andalucía, Murcia, Castilla-La Mancha, Extremadura, Madrid); West (rest of the communities). The letters "W", "S" and "E" mark the location of the three representative sites in the Western, Southern and Eastern regions described in Table 2. (For interpretation of the references to color in this figure legend, the reader is referred to the web version of this article.)

Fig. 4 also shows that the LCOE of FPV can accept slightly higher CAPEX than the NPV. The difference is mainly dictated by the electricity price forecast, whose variations affect the NPV requirements. Indeed, higher electricity price forecasts will "favor" those systems with higher energy yields (LPV for the current assumptions), forcing lower CAPEX for FPV to be cost-competitive. This does not mean that lower energy yield systems (as FPV) will not economically benefit of higher electricity prices, rather that the increase in profits will be lower compared to higher energy yield systems. Therefore, in higher price scenarios, lower yield systems will require even lower CAPEX to balance the reduced increases in revenues and to be still economically competitive with LPV. The results of this analysis are summarized in Fig. 5, where the CAPEX ranges for FPV in the three future electricity trends of Fig. 2 are shown. The average CAPEX for FPV will be 4–5% lower than the 700 €/kW assumed for LPV, depending on the electricity price scenario and the

Table 2
Maximum FPV CAPEX to achieve the same LCOE and NPV than conventional LPV, for the three electricity price scenarios shown in Fig. 2 and three representative locations described in Table 2.

Macro-regions		East, E	South, S	West, W
Autonomous communities		Aragon, Cataluña, Valencia	Andalucía, Murcia, Castilla-La Mancha, Extremadura, Madrid	Rest of the communities
Representative Location		Riba-roja d'Ebre, Cataluña	Puebla de Guzmán, Andalucía	Chantada, Galicia
LCOE CAPEX		668.9	687.1	689.0
LCOE CAPEX variation per degree of tilt		5.1	4.3	4.4
NPV CAPEX	**Low Electricity Price Scenario**	660.3	679.0	684.2
	Intermediate Electricity Price Scenario	651.5	675.1	681.3
	High Electricity Price Scenario	648.2	673.7	680.3
NPV CAPEX variation per degree of tilt		6.9	6.1	5.3

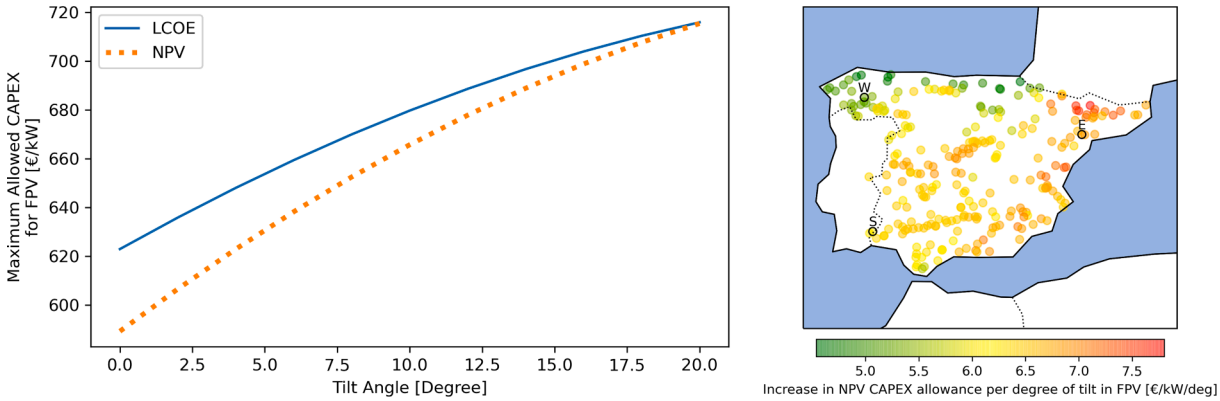

Fig. 6. Left Plot: Maximum FPV CAPEX allowance depending on tilt angle (national average). Right Plot: Variation in NPV CAPEX allowance depending on tilt angle per location. The letters "W", "S" and "E" mark the location of the three representative locations in the Western, Southern and Eastern regions described in Table 2.

location. The Eastern part of Spain will be suffering the most for potential high electricity prices, while the CAPEX reduction will be limited in the Northwest.

One factor that has a significant influence the PV performance is the tilt angle, typically limited for FPV by the wind load that the system can withstand. Taking into account installation costs, soiling losses and wind forces, Silvério et al. (Silvério et al., 2018) recommended tilt angles $\leq 10^{\circ}$ for FPV. In this work, the FPV title angle has been fixed to 10°, the maximum recommended by that study. However, higher energy yields could be achieved thanks to higher tilt angles (El Hammoumi et al., 2021), but these are likely to require additional CAPEX to strengthen the FPV foundations (Silvério et al., 2018). The left plot of Fig. 6 shows how the CAPEX allowance increases with the tilt angle: the higher allowances could be potentially used to cover the supplementary foundations work. At the given conditions, FPV would match the LPV economic performance at tilt angles in between 16° and 18°.

Both trends in Fig. 6 could be approximated to lines ($R^2 > 0.98$). At national level, the LCOE CAPEX allowance increases by 4.7 €/kW per degree of tilt, while the NPV CAPEX by 6.3 €/kW per degree of tilt. However, these rates change depending on the location, with the northeastern regions registering the highest variation: 5.0 €/kW/deg for the LCOE CAPEX and 6.9 €/kW/deg for the NPV CAPEX (right plot of Fig. 6).

3.3. The effect of temperature

As discussed in the previous section, and anticipated by other authors (Rosa-Clot and Tina, 2020c), the lower module temperature could play a fundamental role in the economics of floating PV. The improved thermal performance, indeed, could counter-balance, at least in part, the losses due to the lower tilt angles. So far, the U-value for FPV has been set to 56 W/m^{2}K, result of the review conducted on the studies available in literature. This is the one found by (Dörenkämper et al., 2021) for structures allowing the direct exposure of the backside of the PV modules to the water. It is about twice the 29 W/m^{2}K typically considered for conventional PV systems (PVsyst SA, n.d.). However, FPV systems can be built with several different configurations, each potentially affecting also the thermal exchange between the modules and the environment, and therefore, one can expect this U-value not to be representative for the whole FPV market. Therefore, the analysis was repeated taking into account a range of U-values for FPV going from 29 W/m^{2}K, typically considered for LPV systems (PVsyst SA, n.d.), to 71 W/m^{2}K, the maximum value reported for FPV modules in direct contact with water (Kjeldstad et al., 2021).

The results of the analysis are reported in Fig. 7, where the relation between the maximum allowed CAPEX and the U-value is shown. As expected, higher U-values will favor the thermal exchange, reducing the module temperature and boosting the electrical performance of FPV.

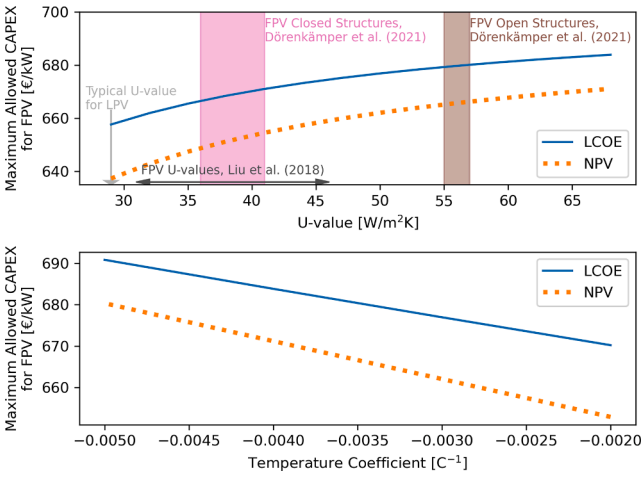

Fig. 7. Upper plot: Maximum allowed CAPEX for FPV to be cost-competitive with LPV depending on the U-value of FPV system. The U-value of LPV is fixed to 29 W/m^{2}K. Experimental U-values reported in literature for FPV systems are shown. Lower plot: Maximum allowed CAPEX for FPV to be cost-competitive with LPV depending on temperature coefficient of the modules. Both LPV and FPV modules are modelled to have the same temperature coefficient. The values shown in both plots are calculated from the simple average of the results obtained for each location.

LCOE and NPV are similarly affected by the thermal behavior, with the CAPEX threshold for FPV increasing by >25 €/kW across the U-value range here considered (29–71 W/m^{2}K). This work takes into account a baseline U-value of 56 W/m^{2}K for FPV, average of those reported by (Dörenkämper et al., 2021) for open structures. The same work reports U-values in between 36 and 41 W/m^{2}K for close structure FPV systems; in these cases, the allowed CAPEX lower by 9–18 €/kW compared to the baseline scenario. If FPV did not experience any thermal benefit (Peters and Nobre, 2020), its CAPEX should be on average 6–9% lower than those of LPV to be cost-competitive. In this case, the highest CAPEX allowances would be in the northwest (649 to 663 €/kW), while the Southern regions would require CAPEX in between 636 and 658 €/kW.

So far, the analysis has modelled a PV module with temperature coefficient of $-0.0034C^{-1}$ (Trina, 2021). This is within the −0.003 to −0.005 range in which 90% of the mono and poly crystalline silicon modules reported in the California Energy Commission list (California Energy Commission, 2021) fall. However, some Silicon modules with temperature coefficients varying from $-0.002C^{-1}$ to $-0.009C^{-1}$ are also present in that list. It is worth therefore analyzing how this coefficient could influence the thermal management of FPV and its economic returns. The results of this analysis, conducted by changing the

temperature coefficient of both FPV and LPV, are shown in the lower plot of Fig. 7. As expected, the lower the temperature coefficient (i.e. the higher its absolute value and, so, the more temperature dependent the module), the better the FPV performance compared to LPV and, therefore, the higher the allowed CAPEX threshold. Decreasing the temperature coefficient by $-0.001C^{-1}$ increases the CAPEX allowance by 7 and 9 €/kW for LCOE and NPV, respectively. However, while the economic gap between FPV and LPV lowers as the temperature coefficient diminishes, this also affects negatively the absolute values of LCOE and NPV. Indeed lower temperature coefficients will reduce the average energy yield of PV: at national level, LPV loses 15 kWh/kW/year and FPV loses 2 kWh/kW/year per $0.001C^{-1}$ decrease in temperature coefficient. It is because of this limited loss that the FPV CAPEX increases while the temperature coefficient decreases.

3.4. Discussion

Despite the growing interest in floating-PV, the information on the performance and the economics of these systems is often still design-specific. Therefore, some assumptions had to be made in this analysis. In particular, the annual O&M costs (OMEX) of land based and floating PV systems have been considered the same. In their review, Sahu et al. (Sahu et al., 2016) stated that the FPV OMEX are often lower than land-based PV, because "the water needed for cleaning is available at source and components are less likely to overheat". In addition, they added that no maintenance is required to remove vegetation and dust deposition is expected to be less severe than for LPV. However, bird dropping might actually occur more frequently on floating modules (Liu et al., 2018), potentially requiring the FPV systems to be cleaned more often. In addition to the higher frequency, cleanings, as well as other maintenance operations, might be also more expensive than in LPV. Indeed, these activities might be more difficult to realize, might require more time, might need water vehicles or might have to be conducted under the water surface, potentially increasing the OMEX (Gorjian et al., 2021). Oliveira-Pinto and Stokkermans (Oliveira-Pinto and Stokkermans, 2020) "conservatively" assumed OMEX costs equal to 10% of the CAPEX for FPV and to 1.5% of the CAPEX for land based PV. Fereshtehpour et al. (Fereshtehpour et al., 2021) reported OMEX costs for FPV between 2 and 4% higher than LPV in Iran. Additional field data should be shared in future to identify more clearly the extent and the trends of OMEX in FPV as their actual value will have an impact on the economics of FPV. In addition, in some cases, expenditures such as the land fees are included in the OMEX rather than in the CAPEX. So, the present economic investigation was extended to include also a sensitivity analysis on the influence of OMEX on the FPV economics. In this case the OMEX of FPV were varied from 5 €/kW/year to 25 €/kW/year keeping the LPV ones at 15 €/kW/year, as in (Talavera et al., 2019). As shown in Fig. 8A, both LCOE and NPV CAPEX allowances of FPV were found to increase linearly while OMEX lowered: each additional 1 €/kW spent per year on OMEX in FPV reduces the CAPEX allowance by ~13 €/kW.

A second factor that was not taken into account in the previous analysis was the reduction in water evaporation rates achievable with FPV. Evaporation water savings can potentially lead to two economic benefits:

- Hydroelectric plants might use that additional water to produce more electricity.
- Saved water can be used (and resold) for irrigation or other purposes.

However, the evaporation savings are related to the design of the systems. Designs that favor ventilation and evaporative cooling will likely lower the module temperature, but reduce also the evaporation savings (Bontempo Scavo et al., 2021). An analysis showed that covering about 1% of the largest African reservoirs could lead to the generation of additional 0.3% hydropower electricity on top of the FPV output thanks to evaporation savings (Gonzalez Sanchez et al., 2021). Fig. 8B shows the variation in the CAPEX requirement achievable thanks to the extra-hydroelectric energy generation. It is found that the CAPEX requirement increases linearly with the percentage of extra energy, with NPV's CAPEX and the LCOE's CAPEX increasing by 11.3 €/kW and by 8.7 €/kW per point of additional hydroelectric energy production, respectively.

Scarce data are nowadays available on FPV degradation. While the enhanced thermal exchange might reduce thermal degradation (Rosa-Clot and Tina, 2020c), researchers agree that the challenging water environment can pose risks on FPV systems, especially over the long run (Gorjian et al., 2021). Liu et al. (Liu et al., 2018) listed a number of possible issues that can affect the performance, which included potential induced degradation, corrosion and failure of anchoring and mooring structures. A recent work conducted on a FPV system installed in West Bengal, India (Goswami and Sadhu, 2021), showed similar degradation rates for FPV and LPV modules (1.18%/year vs. 1.07%/year), over a period of 17 months. Despite the short period, the authors reported that a visual inspection already revealed signs of water-based corrosion and moisture ingression on the FPV modules. In a different work, Luo et al. (Luo et al., 2021) did not find any significant difference in performance loss rate between the modules of a FPV testbed in Singapore and nearby roof-mounted modules. So far, the present analysis considered the same degradation rates for FPV and LPV. Fig. 8C presents a sensitivity analysis where the required FPV CAPEX is recalculated for various degradation rates of the FPV, keeping the LPV degradation rate at 1%/year. In this case, the FPV degradation should be <0.8%/year to match the LPV CAPEX. On the other hand, worsening the degradation by 0.1%/year compared to LPV would cost in between 7.5 and 10.9 €/kW of CAPEX.

In addition, it should be noted that the PV market is experiencing a significant shift toward bifaciality. Bifacial modules can collect light from both the front and the rear sides, increasing the total absorbed irradiance. Their market share is expected to grow beyond 50% by 2030

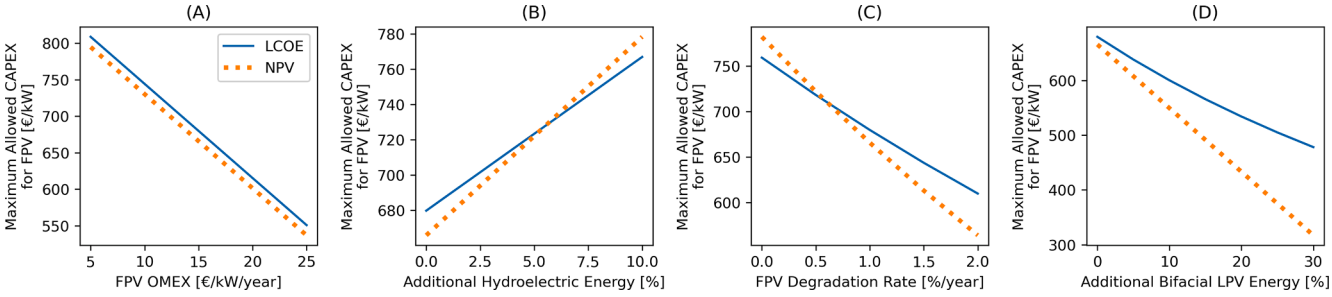

Fig. 8. Sensitivity Analysis. A) FPV maximum CAPEX allowances depending on OMEX, considering fixed 15 €/kW/year OMEX for LPV. B) FPV maximum CAPEX allowances depending on extra hydroelectric generation (relative to FPV generation). C) FPV maximum CAPEX allowances depending on FPV expected degradation rate, considering a fixed 1%/year degradation for LPV. D) FPV maximum CAPEX allowances depending on surplus energy produced by LPV due to bifaciality, considering no improvements in the FPV yield. One parameter only is varied per plot, keeping the LPV CAPEX at 700 €/kW. All the other parameters are set as in Table 1. The values shown in the plots are calculated from the simple average of the results obtained for all locations.

(VDMA, 2021). While the potential and the advantages of bifacial modules in LPV applications are well known (Rodríguez-Gallegos et al., 2020; Sun et al., 2018), only a limited number of studies have investigated the performance of bifacial modules in FPV installations. Most of them shared concerns regarding the low albedo of water compared to land. Liu et al. (Liu et al., 2018) reported no yield improvement for bifacial on water compared to monofacial. Ziar et al. (Ziar et al., 2021) recommended installing reflectors on the floaters and employing horizontal tracking to maximize the performance of bifacial FPV. However, the authors also reported a drop in the reflectors' albedo from 68% to 24% in just 8 months of operation because of bird dropping. The importance of the albedo was also showed by (Tina et al., 2021) which reported increase in FPV yields up to 13.5% for bifacial modules compared to monofacial modules, if the albedo could be raised up to 20%. Additional studies are therefore needed to understand and maximize the performance of bifacial modules in FPV and analyze their cost competiveness compared LPV applications. Indeed, if the advantages of bifacial modules could not be transferred to FPV, the CAPEX allowances for FPV would be substantially lowered (Fig. 8D).

Overall, the results of this work prove that FPV can already compete economically with conventional LPV. However, its profitability and cost still vary with a number of factors, which depends on both the location and the system design. In addition, further parameters can have a role in the energy generation process of FPV and their contribution should be analyzed in the future. Also different FPV configurations should be considered, as the use of trackers and/or cooling systems (Campana et al., 2019; Rosa-Clot and Tina, 2020d) can impact the performance of FPV and LPV and change the FPV CAPEX requirement. All these variables should be taken into account in future studies.

4. Conclusions

This work analyzes the cost competiveness and the profitability of FPV compared to LPV. In particular, the aim is to provide economic targets that FPV developers and installers could use to maximize their profits and minimize the cost of electricity. The comparative analysis takes into account 10° tilt FPV and fixed optimally tilted LPV in Spain, and investigates the impact of different factors and scenarios on the economics of FPV.

An assessment of the potential FPV capacity in Spain is first presented. It is found that FPV can significantly support the renewable shift of the Spanish electricity market. Covering 1% of reservoir surface with PV could add 3 GW to the national photovoltaic capacity and could generate the equivalent of 1.7% of the current national electricity demand. If FPV were built to match the current hydroelectric capacity, it would cover more than 70% of the PV capacity currently missing to reach the 2030 targets and could provide 12% of the national energy demand.

The results of the economic analysis, based on the previously reported U-values of 56 W/m^2K and 29 W/m^2K for FPV and LPV systems respectively, shows that Spanish FPV systems should have CAPEX in between 1 and 10% lower than LPV plants to match their LCOE and NPV. FPV is found to be already competitive in the southernmost regions, where the irradiance and the ambient temperature values are the highest. Temperature plays a key role in the economics of FPV: higher CAPEX investments are indeed allowed in the regions experiencing the highest ambient temperatures. In addition, higher CAPEX would be allowed for FPV systems achieving better thermal exchange abilities, here modelled through higher U-values. Additional factors can loosen the expenditure requirements for FPV, such as water evaporation savings or lower O&M costs. Degradation will also affect the economics of FPV, but additional and long-term data are still needed before drawing any conclusion. Last, the growing deployment of bifacial modules can negatively affect the cost competiveness of FPV, if these lead to no or limited energy yield improvements in FPV applications.

This work makes use of referenced parameters to model the energy and economic performance of the FPV and LPV systems in Spain. However, the developed model could be used to assess the economics of FPV in different regions. The results could be of use in FPV design stage to evaluate pros and cons of various configurations and modules. Given the few FPV information currently available in literature, the model and the results should be also refined in future as new FPV data become available. In addition, more factors and system configurations should be taken into account.

Declaration of Competing Interest

The author declares that he has no known competing financial interests or personal relationships that could have appeared to influence the work reported in this paper.

References

Álvarez, C., Zafra, M., 2021. Cuánto ocupan las megacentrales solares: investigadores alertan del impacto del 'boom' fotovoltaico. El País.

Aparicio, L., 2020. Los agricultores se frotan las manos 'plantando' paneles solares. El País.

Bontempo Scavo, F., Tina, G.M., Gagliano, A., Nižetić, S., 2021. An assessment study of evaporation rate models on a water basin with floating photovoltaic plants. Int. J. Energy Res. 45 (1), 167–188. https://doi.org/10.1002/er.v45.110.1002/er.5170.

BP p.l.c., 2021. bp Statistical Review of World Energy 2021. London, UK.

Buchhorn, M., Lesiv, M., Tsendbazar, N.-E., Herold, M., Bertels, L., Smets, B., 2020. Copernicus global land cover layers—collection 2. Remote Sens. 12, 1044. https://doi.org/10.3390/rs12061044.

California Energy Commission, 2021. Solar Equipment Lists [WWW Document]. URL https://www.energy.ca.gov/programs-and-topics/programs/solar-equipment-lists#accordion-7491 (accessed 5.11.21).

Campana, P.E., Wästhage, L., Nookuea, W., Tan, Y., Yan, J., 2019. Optimization and assessment of floating and floating-tracking PV systems integrated in on- and off-grid hybrid energy systems. Sol. Energy 177, 782–795. https://doi.org/10.1016/j.solener.2018.11.045.

Capellán-Pérez, I., de Castro, C., Arto, I., 2017. Assessing vulnerabilities and limits in the transition to renewable energies: land requirements under 100% solar energy scenarios. Renew. Sustain. Energy Rev. 77, 760–782. https://doi.org/10.1016/j.rser.2017.03.137.

Cazzaniga, R., Rosa-Clot, M., Rosa-Clot, P., Tina, G.M., 2019. Integration of PV floating with hydroelectric power plants. Heliyon 5 (6), e01918. https://doi.org/10.1016/j.heliyon.2019.e01918.

Copernicus Atmosphere Monitoring Service, n.d. CAMS solar radiation time-series [WWW Document]. URL https://ads.atmosphere.copernicus.eu/ (accessed 11.9.20).

Cromratie Clemons, S.K., Salloum, C.R., Herdegen, K.G., Kamens, R.M., Gheewala, S.H., 2021. Life cycle assessment of a floating photovoltaic system and feasibility for application in Thailand. Renew. Energy 168, 448–462. https://doi.org/10.1016/j.renene.2020.12.082.

De Soto, W., Klein, S.A., Beckman, W.A., 2006. Improvement and validation of a model for photovoltaic array performance. Sol. Energy 80 (1), 78–88. https://doi.org/10.1016/j.solener.2005.06.010.

Deboutte, G., 2021. Thailand's first floating PV project goes online. pv-magazine.

Dobos, A.P., 2014. PVWatts Version 5 Manual.

Dörenkämper, M., Wahed, A., Kumar, A., de Jong, M., Kroon, J., Reindl, T., 2021. The cooling effect of floating PV in two different climate zones: a comparison of field test data from the Netherlands and Singapore. Sol. Energy 219, 15–23. https://doi.org/10.1016/j.solener.2021.03.051.

El Hammoumi, A., Chalh, A., Allouhi, A., Motahhir, S., El Ghzizal, A., Derouich, A., 2021. Design and construction of a test bench to investigate the potential of floating PV systems. J. Clean. Prod. 278, 123917. https://doi.org/10.1016/j.jclepro.2020.123917.

Faiman, D., 2008. Assessing the outdoor operating temperature of photovoltaic modules. Prog. Photovoltaics Res. Appl. 16 (4), 307–315. https://doi.org/10.1002/pip.v16:410.1002/pip.813.

Fang, W., Huang, Q., Huang, S., Yang, J., Meng, E., Li, Y., 2017. Optimal sizing of utility-scale photovoltaic power generation complementarily operating with hydropower: a case study of the world's largest hydro-photovoltaic plant. Energy Convers. Manag. 136, 161–172. https://doi.org/10.1016/j.enconman.2017.01.012.

Fereshtehpour, M., Javidi Sabbaghian, R., Farrokhi, A., Jovein, E.B., Ebrahimi Sarindizaj, E., 2021. Evaluation of factors governing the use of floating solar system: a study on Iran's important water infrastructures. Renew. Energy 171, 1171–1187. https://doi.org/10.1016/j.renene.2020.12.005.

Ferrer-Gisbert, C., Ferrán-Gozálvez, J.J., Redón-Santafé, M., Ferrer-Gisbert, P., Sánchez-Romero, F.J., Torregrosa-Soler, J.B., 2013. A new photovoltaic floating cover system for water reservoirs. Renew. Energy 60, 63–70. https://doi.org/10.1016/j.renene.2013.04.007.

Ford, N., 2019. Merchant appetite boosts Spanish solar boom but cost risks lurk. Reuters Events.

Fox, R., n.d. Global - Dams Database [WWW Document]. URL https://datacatalog.worldbank.org/dataset/global-dams-database (accessed 5.10.21).

Gobierno de España, 2020. Plan de Energía Nacional Integrada y Climática de España.

Gonzalez Sanchez, R., Kougias, I., Moner-Girona, M., Fahl, F., Jäger-Waldau, A., 2021. Assessment of floating solar photovoltaics potential in existing hydropower reservoirs in Africa. Renew. Energy 169, 687–699. https://doi.org/10.1016/j.renene.2021.01.041.
Gorjian, S., Sharon, H., Ebadi, H., Kant, K., Scavo, F.B., Tina, G.M., 2021. Recent technical advancements, economics and environmental impacts of floating photovoltaic solar energy conversion systems. J. Clean. Prod. 278, 124285. https://doi.org/10.1016/j.jclepro.2020.124285.
Goswami, A., Sadhu, P.K., 2021. Degradation analysis and the impacts on feasibility study of floating solar photovoltaic systems. Sustain. Energy, Grids Networks 26, 100425. https://doi.org/10.1016/j.segan.2020.100425.
Gschwind, B., et al., 2019. Improving the McClear model estimating the downwelling solar radiation at ground level in cloud free conditions – McClear-V3., Meteorol. Z., http://doi.org/10.1127/metz/2019/0946.
Haugwitz, F., 2020. Floating solar PV gains global momentum. PV Mag. Int. 1–10.
Hay, J.E., Davies, J.A., 1980. Calculations of the solar radiation incident on an inclined surface. In: Proceedings of the 1st Canadian Solar Radiation Data Workshop. Toronto, Canada.
Holmgren, W.F., Hansen, C.W., Mikofski, M.A., 2018. pvlib python: a python package for modeling solar energy systems. J. Open Source Softw. 3 (29), 884. https://doi.org/10.21105/joss10.21105/joss.00884.
IEA PVPS, 2020. Trends in photovoltaic applications 2019.
Inness, A., et al., 2019. The CAMS reanalysis of atmospheric composition. Atmos. Chem. Phys. 19, 3515–3556.
IRENA, 2020. Renewable Power Generation Costs in 2020. Abu Dhabi.
Jiménez-Castillo, G., Muñoz-Rodriguez, F.J., Rus-Casas, C., Talavera, D.L., 2020. A new approach based on economic profitability to sizing the photovoltaic generator in self-consumption systems without storage. Renew. Energy 148, 1017–1033. https://doi.org/10.1016/j.renene.2019.10.086.
Kjeldstad, T., Lindholm, D., Marstein, E., Selj, J., 2021. Cooling of floating photovoltaics and the importance of water temperature. Sol. Energy 218, 544–551. https://doi.org/10.1016/j.solener.2021.03.022.
Lee, N., Grunwald, U., Rosenlieb, E., Mirletz, H., Aznar, A., Spencer, R., Cox, S., 2020. Hybrid floating solar photovoltaics-hydropower systems: benefits and global assessment of technical potential. Renew. Energy 162, 1415–1427. https://doi.org/10.1016/j.renene.2020.08.080.
Lefèvre, M., et al., 2013. McClear: a new model estimating downwelling solar radiation at ground level in clear-sky conditions. AMT 6, 2403–2418. https://doi.org/10.5194/amt-6-2403-2013.
Lehner, B., Liermann, C.R., Revenga, C., Vörömsmarty, C., Fekete, B., Crouzet, P., Döll, P., Endejan, M., Frenken, K., Magome, J., Nilsson, C., Robertson, J.C., Rödel, R., Sindorf, N., Wisser, D., 2011. High-resolution mapping of the world's reservoirs and dams for sustainable river-flow management. Front. Ecol. Environ. https://doi.org/10.1890/100125.
Lightsource bp, 2016. Queen Elizabeth II Reservoir Solar Project [WWW Document]. URL https://www.lightsourcebp.com/uk/projects/queen-elizabeth-ii-reservoir-solar-project/ (accessed 5.11.21).
Liu, H., Krishna, V., Lun Leung, J., Reindl, T., Zhao, L., 2018. Field experience and performance analysis of floating PV technologies in the tropics. Prog. Photovoltaics Res. Appl. 26 (12), 957–967. https://doi.org/10.1002/pip.v26.1210.1002/pip.3039.
Loutzenhiser, P.G., Manz, H., Felsmann, C., Strachan, P.A., Frank, T., Maxwell, G.M., 2007. Empirical validation of models to compute solar irradiance on inclined surfaces for building energy simulation. Sol. Energy 81 (2), 254–267. https://doi.org/10.1016/j.solener.2006.03.009.
Luo, W., Isukapalli, S.N., Vinayagam, L., Ting, S.A., Pravettoni, M., Reindl, T., Kumar, A., 2021. Performance loss rates of floating photovoltaic installations in the tropics. Sol. Energy 219, 58–64. https://doi.org/10.1016/j.solener.2020.12.019.
Mazzoni, M., Manuell, R., 2019. Long-term power market outlook in Europe, in: ICIS Energy Forum 2019. ICIS – Independent Commodity Intelligence Services.
Micheli, L., Solas, Á.F., Soria-Moya, A., Almonacid, F., Fernández, E.F., 2021. Short-term impact of the COVID-19 lockdown on the energy and economic performance of photovoltaics in the Spanish electricity sector. J. Clean. Prod. 308, 127045. https://doi.org/10.1016/j.jclepro.2021.127045.
Micheli, L., Theristis, M., Talavera, D.L., Almonacid, F., Stein, J.S., Fernández, E.F., 2020. Photovoltaic cleaning frequency optimization under different degradation rate patterns. Renew. Energy 166, 136–146. https://doi.org/10.1016/j.renene.2020.11.044.
Molina, P.S., 2020. Floating PV gains ground in Iberia. In: PV RES Conf.
Mulligan, M., van Soesbergen, A., Sáenz, L., 2020. GOODD, a global dataset of more than 38,000 georeferenced dams. Sci. Data 7, 1–8. https://doi.org/10.1038/s41597-020-0362-5.
Oliveira-Pinto, S., Stokkermans, J., 2020. Assessment of the potential of different floating solar technologies – Overview and analysis of different case studies. Energy Convers. Manag. 211, 112747. https://doi.org/10.1016/j.enconman.2020.112747.
OMIE, n.d. Mínimo, medio y máximo precio mercado diario [WWW Document]. URL www.omie.es.
Padilha Campos Lopes, M., de Andrade Neto, S., Alves Castelo Branco, D., Vasconcelos de Freitas, M.A., da Silva Fidelis, N., 2020. Water-energy nexus: floating photovoltaic systems promoting water security and energy generation in the semiarid region of Brazil. J. Clean. Prod. 273, 122010. https://doi.org/10.1016/j.jclepro.2020.122010.
Perez-Linkenheil, C., 2019. Update December 2019 – EU Energy Outlook 2050 [WWW Document]. Energy Brainpool. (accessed 4.15.21) https://blog.energybrainpool.com/en/update-december-2019-eu-energy-outlook-2050/.
Peters, I.M., Nobre, A.M., 2020. On module temperature in floating PV systems. In: Conf. Rec. IEEE Photovolt. Spec. Conf. 2020-June, 0238–0241. https://doi.org/10.1109/PVSC45281.2020.9300426.
PVsyst SA, n.d. PVsyst [WWW Document]. URL https://www.pvsyst.com/ (accessed 5.6.21).
Qu, Z., et al., 2017. Fast radiative transfer parameterisation for assessing the surface solar irradiance: The Heliosat-4 method. Meteorol. Z. 26, 33–57. https://doi.org/10.1127/metz/2016/0781.
REE, 2020. National statistical series [WWW Document]. accessed 7.28.20. https://www.ree.es/en/datos/publications/national-statistical-series.
Rodríguez-Gallegos, C.D., Liu, H., Gandhi, O., Singh, J.P., Krishnamurthy, V., Kumar, A., Stein, J.S., Wang, S., Li, L., Reindl, T., Peters, I.M., 2020. Global techno-economic performance of bifacial and tracking photovoltaic systems. Joule 4 (7), 1514–1541. https://doi.org/10.1016/j.joule.2020.05.005.
Rollet, C., 2020. Baywa's plans for floating PV. pv-magazine.
Rosa-Clot, M., Tina, G.M., 2020a. Current status of FPV and trends, Floating PV Plants. Elsevier Inc. https://doi.org/10.1016/B978-0-12-817061-8.00002-6.
Rosa-Clot, M., Tina, G.M., 2020b. Introduction, Floating PV Plants. Elsevier Inc. https://doi.org/10.1016/B978-0-12-817061-8.00001-4.
Rosa-Clot, M., Tina, G.M., 2020c. Levelized cost of energy (LCOE) analysis, Floating PV Plants. Elsevier Inc. https://doi.org/10.1016/B978-0-12-817061-8.00010-5.
Rosa-Clot, M., Tina, G.M., 2020d. Cooling systems, Floating PV Plants. Elsevier Inc. https://doi.org/10.1016/B978-0-12-817061-8.00006-3.
Sahu, A., Yadav, N., Sudhakar, K., 2016. Floating photovoltaic power plant: a review. Renew. Sustain. Energy Rev. 66, 815–824. https://doi.org/10.1016/j.rser.2016.08.051.
Serrano, D., Margalida, A., Pérez-García, J.M., Juste, J., Traba, J., Valera, F., Carrete, M., Aihartza, J., Real, J., Mañosa, S., Flaquer, C., Garin, I., Morales, M.B., Alcalde, J.T., Arroyo, B., Sánchez-Zapata, J.A., Blanco, G., Negro, J.J., Tella, J.L., Ibañez, C., Tellería, J.L., Hiraldo, F., Donázar, J.A., 2020. Renewables in Spain threaten biodiversity. Science (80-.) 370 (6522), 1282–1283. https://doi.org/10.1126/science:abf6509.
Silvério, N.M., Barros, R.M., Tiago Filho, G.L., Redón-Santafé, M., Santos, I.F.S. dos, Valério, V.E. de M., 2018. Use of floating PV plants for coordinated operation with hydropower plants: case study of the hydroelectric plants of the São Francisco River basin. Energy Convers. Manag. 171, 339–349. https://doi.org/10.1016/j.enconman.2018.05.095.
Sun, X., Khan, M.R., Deline, C., Alam, M.A., 2018. Optimization and performance of bifacial solar modules: a global perspective. Appl. Energy 212, 1601–1610. https://doi.org/10.1016/j.apenergy.2017.12.041.
Talavera, D.L., Muñoz-Cerón, E., Ferrer-Rodríguez, J.P., Pérez-Higueras, P.J., 2019. Assessment of cost-competitiveness and profitability of fixed and tracking photovoltaic systems: the case of five specific sites. Renew. Energy 134, 902–913. https://doi.org/10.1016/j.renene.2018.11.091.
Taylor, S.J., Letham, B., 2017. Forecasting at scale. PeerJ Prepr. https://doi.org/10.7287/peerj.preprints.3190v2.
Theristis, M., Livera, A., Jones, C.B., Makrides, G., Georghiou, G.E., Stein, J.S., 2020. Nonlinear photovoltaic degradation rates: modeling and comparison against conventional methods. IEEE J. Photovoltaics 10 (4), 1112–1118. https://doi.org/10.1109/JPHOTOV.550386910.1109/JPHOTOV.2020.2992432.
Tina, G.M., Bontempo Scavo, F., Merlo, L., Bizzarri, F., 2021. Comparative analysis of monofacial and bifacial photovoltaic modules for floating power plants. Appl. Energy 281, 116084. https://doi.org/10.1016/j.apenergy.2020.116084.
Trina, 2021. Vertex TSM-DE20 585-605W.
VDMA, 2021. International Technology Roadmap for Photovoltaic (Results 2020). Frankfurt am Main, Germany.
World Bank Group, ESMAP, SERIS, 2018. Where Sun Meets Water: Floating Solar Market Report—Executive Summary, Where Sun Meets Water. Washington, DC. https://doi.org/10.1596/31880.
Ziar, H., Prudon, B., Lin, F.V., Roeffen, B., Heijkoop, D., Stark, T., Teurlincx, S., Senerpont Domis, L., Goma, E.G., Extebarria, J.G., Alavez, I.N., Tilborg, D., Laar, H., Santbergen, R., Isabella, O., 2021. Innovative floating bifacial photovoltaic solutions for inland water areas. Prog. Photovoltaics Res. Appl. 29 (7), 725–743. https://doi.org/10.1002/pip.v29.710.1002/pip.3367.